Electronic transport properties of carbon nanotube metal-semiconductor-metal

F Khoeini and H Farman

Department of Physics, Iran University of Science and Technology (IUST), Narmak, 16846, Tehran, Iran

Abstract

In this work, we study electronic transport properties of a quasi-one dimensional pure semi-conducting Zigzag Carbon Nanotube (CNT) attached to semi-infinite clean metallic Zigzag CNT leads, taking into account the influence of topological defect in junctions. This structure may behave like a field effect transistor. The calculations are based on the tight-binding model and Green's function method, in which the local density of states(LDOS) in the metallic section to semi-conducting section, and muli-channel conductance of the system are calculated in the coherent and linear response regime, numerically. Also we have introduced a circuit model for the system and investigated its current. The theoretical results obtained, can be a base, for developments in designing nano-electronic devices.

Keywords: carbon nanotubes, electronic transport, AC current

1. Introduction

Since the discovery of carbon nanotubes (CNTs) in 1991[1], the studies on the properties of various nanometer-scale tubular structures and their synthesis have never been stopped. Due to the development of micro-manufacture technology, miniaturization of microelectronic devices has led to intense research directed towards the development of molecular electronics [2,3]. The unique electrical and mechanical properties of carbon nanotubes have stimulated these efforts, because CNTs, especially single-walled carbon nanotubes (SWCNTs), exhibit a range of suitable properties for nano devices. To date, many basic micro- electronic devices based on SWCNTs, such as molecular wires, diodes, and field-effect transistors, have been invented. The study of transport through molecular junctions is an important topic in nanotechnology. SWCNTs are also interesting in this context: they are stable; they can be easily manipulated; they can be contacted to external leads; they can be both metallic and semiconducting depending on the diameter and helicity of their atomic structure. The possibility of realizing seamless connections between SWCNTs with different helicities has been stimulated. Metal-semiconductor junctions with simple interfaces can be obtained in this way. Rectifying current properties, similar to diodes, are predictable for these systems. A simple end to end connection between two different nanotubes, known as intra-molecular junction, can be realized by the incorporation of an equal number of pentagons and heptagons, just a single pair in the simplest case [4,5]. More complex structures can be formed, still by incorporating pentagons and heptagons in the otherwise perfect honeycomb arrangement of the carbon atoms.

Intra-molecular junctions are ideal systems for the study of the electronic structure of metal-semiconductor [6–8], metal-metal [9], and semiconductor-semiconductor [10] interfaces, to investigate the Schottky barrier formation in such junctions [11, 12], and to calculate their transport properties [13-15]. By combining two intra-molecular junctions in series, a quantum dot can be obtained when the metallic part is sandwiched between two semiconducting nanotubes [16]. Metal-semiconductor-metal structure may behave like a field effect transistor.

The purpose of this article is to analyze numerically the electronic structure, conductance and obtaining the circuit model for the system. A semi-conducting tube of helicity (11, 0) is sandwiched between two semi-infinite metallic tubes of helicity (12, 0). The system is represented in figure 1. Each (12, 0)–(11, 0) junction includes a single pentagon–heptagon pair.

2. Description of model and method

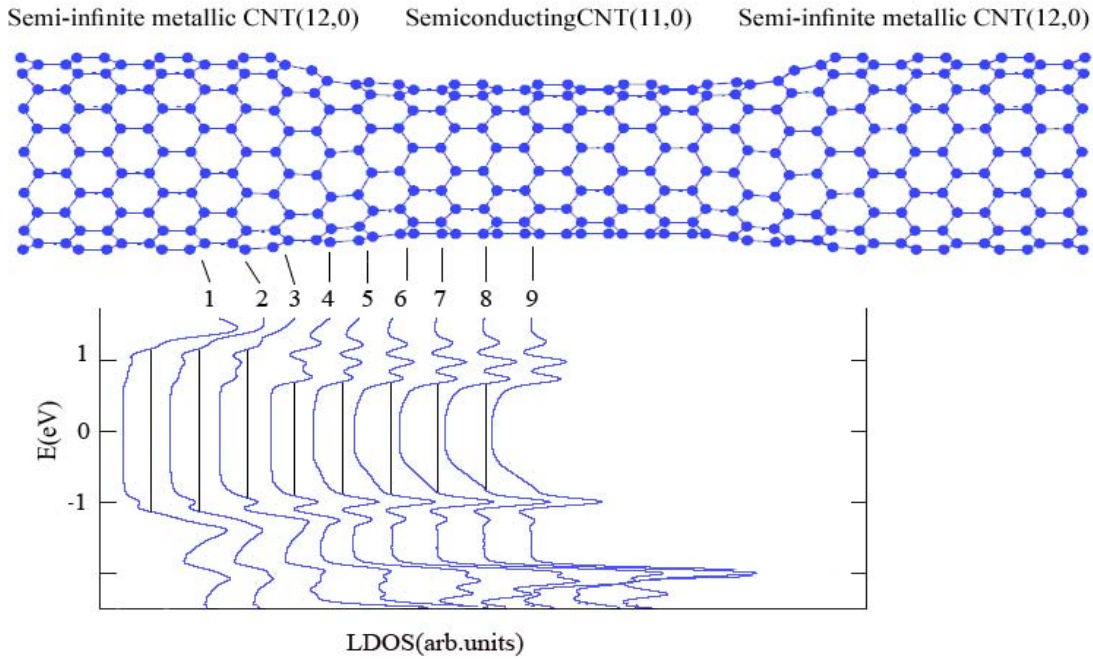In this section, we study the electronic transport in a

Figure 1. Carbon nanotube metal-semiconductor-metal (12, 0)–(11, 0)–(12, 0) with a five-unit-cell along (11, 0) and local density of states diagram for nine zigzag rings on interface [7].

quasi-one-dimensional structure formed of N atomic rings connected to two semi-infinite order metallic leads.

The geometrical structure under consideration is composed of two CNT leads plus semi-conducting CNT section, which can be described by a tight-binding Hamiltonian with one π electron per atom. The tight-binding Hamiltonian of a CNT is written as

$$H = \sum_j |\pi_j\rangle \varepsilon_j \langle \pi_j| + \gamma_\circ \sum_{<i,j>} |\pi_j\rangle \langle \pi_i|, \qquad (1)$$

where the sum over i, j is restricted to the nearest-neighbor site, and $\gamma_0 = -2.7$ eV. On site energies, ε_j, are set to zero. We divide the structure of CNT, into smaller units, each unit typically representing one ring of atoms along the circumference of the tube. For a (n, 0) zigzag CNT, there are n carbon atoms in each ring and a total of N atoms in the entire CNT. If we use $|L\rangle$ to represent the basis state for the L th ring of the CNT, then Schrödinger equation for the eigenfunction,

$|\Psi\rangle = \sum_L \psi_L |L\rangle$, can be determined by

$\beta_{L+1}\psi_{L+1} + \beta_{L-1}\psi_{L-1} + \alpha_L\psi_L = E\psi_L$ where $n \times n$ matrix β_{L+1} is the interaction Hamiltonian between two neighboring rings and $n \times n$ matrix α_L is the Hamiltonian of the L th ring. The potential can be invariant around CNT, so

$$[\alpha_L] = \varepsilon_L [I]. \qquad (2)$$

For a zigzag tube, β_{L+1} is either β_1 or β_2. Therefore, $n \times n$ matrix of β_1 is $\left[\beta_1 \right] = \gamma_0 [I]$ and for β_2 is:

$$[\beta_2] = \gamma_0 \begin{bmatrix} 1 & & \dots & 1 \\ 1 & 1 & & \\ & 1 & 1 & \\ & \dots & \dots & \end{bmatrix}. \qquad (3)$$

The Hamiltonian matrix for the CNT is the block tridiagonal:

$$H_{1,2,S} = \begin{bmatrix} \alpha_1 & \beta_2^+ & & & \\ \beta_2 & \alpha_2 & \beta_1 & & \\ & \beta_1 & \alpha_3 & \beta_2 & \\ & & \dots & & \\ & & & \dots & \end{bmatrix} \qquad (4)$$

The Hamiltonian of system can be divided in three blocks corresponding to the semi-conducting system S and two periodic semi-infinite metallic carbon nanotubes 1 and 2:

$$H = \begin{bmatrix} H_1 & H_{1S} & 0 \\ H_{1S}^+ & H_S & H_{2S}^+ \\ 0 & H_{2S} & H_2 \end{bmatrix}, \qquad (5)$$

Sub-matrices H_S, H_1 and H_2 respectively describe the semi-conducting and the metallic CNTs. H_{1S} and H_{2S} is the coupling matrix between the left(right) CNT and the semi-conducting CNT. Local density of states and conductance of the system are calculated within the Green's function formalism. The Green's function for the whole system is:

$$G(E) = [(E + i\eta)I - H]^{-1}, \qquad (6)$$

where η, is an arbitrarily small number added into the

above equation to incorporate the convergence conditions and I is the identity matrix. The retarded and advanced Green's function for the coupled semi-conducting CNT in the subspace of G is [17]:

$$G^{r,a}(E) = [(E + i\eta)I - H_S - \sum\nolimits_1^{r,a}(E) - \sum\nolimits_2^{r,a}(E)]^{-1},$$

(7)

where $\sum_1^{r,a}(E)$ and $\sum_2^{r,a}(E)$ are the self-energy terms which can be viewed as effective Hamiltonians that arise from the coupling of the system S with the CNT leads. We divide the system into principal layers with nearest-neighbor interactions. This corresponds to transforming the original system into a linear chain of principal layers. Within this approach, the matrix elements of (6) between layers will yield a set of equations for the Green's functions:

$$[(E + i\eta)I - H_{00}]G_{00} = I + H_{01}G_{10},$$

$$[(E + i\eta)I - H_{00}]G_{10} = H_{01}^+G_{00} + H_{01}G_{20},$$

(8)

$$[(E + i\eta)I - H_{00}]G_{n0} = H_{01}^+G_{n-1,0} + H_{01}G_{n+1,0},$$

where H_{nm} and G_{nm} are the matrix elements of the Hamiltonian and the Green's function between the layer orbitals. Following the method of references [14, 18-20], we obtain $\sum_1^r(E) = H_{1S}^+\overline{T}$ and $\sum_2^r(E) = H_{2S}T$. Here

T and $\overline{T}$ are the transfer matrices, which are calculated from the Hamiltonian matrix elements via an iterative procedure:

$$T = t_0 + \tilde{t}_0 t_1 + \tilde{t}_0 \tilde{t}_1 t_2 + \ldots + \tilde{t}_0 \tilde{t}_1 t_2 \ldots t_n,$$

(9)

$$\overline{T} = \tilde{t}_0 + t_0 \tilde{t}_1 + t_0 t_1 \tilde{t}_2 + \ldots + t_0 t_1 t_2 \ldots \tilde{t}_n,$$

(10)

where t_i and $\tilde{t}_i$ are introduced via the recursion formulas

$$t_i = (I - t_{i-1}\tilde{t}_{i-1} - \tilde{t}_{i-1}t_{i-1})^{-1}t_{i-1}^2,$$

(11)

$$\tilde{t}_i = (I - t_{i-1}\tilde{t}_{i-1} - \tilde{t}_{i-1}t_{i-1})^{-1}\tilde{t}_{i-1}^2,$$

(12)

$$t_0 = [(E + i\eta)I - H_{00}]^{-1}H_{1S}^+,$$

(13)

$$\tilde{t}_0 = [(E + i\eta)I - H_{00}]^{-1}H_{01}.$$

(14)

The process is repeated until $t_n, \tilde{t}_n \leq \delta$ with arbitrarily small. We obtain the average LDOS at ring j and at the energy E by

$$\rho_L(E) = -1 / (\pi n_L) \operatorname{Im}TrG_{L,L}(E),$$

(15)

where T stands for the trace over the n_L carbon atoms of ring L and $G_{L,L}(E)$, is the Lth diagonal sub-matrix of the Green's function of the system. In coherent regime and linear response approach, the low bias multi–channel conductance Γ is calculated by just evaluating transmission function at the Fermi energy [17, 21-23],

$$\Gamma = \Gamma_0 T(E_F),$$

(16)

$$T = Tr[\Gamma_1 G^r \Gamma_2 G^a],$$

(17)

where $\Gamma_0 = \dfrac{2e^2}{h}$ and T are quantum conductance and transmission function of an electron crossing through the system, at the Fermi energy. The matrices G^r, G^a are the retarded and advanced Green functions inside the system S, and $\Gamma_{1,2}(E)$ are the coupling of the semi-conducting CNT to the leads. The matrices $\Gamma_{1,2}(E)$, also given by [17] are:

$$\Gamma_{1,2}(E) = i[\sum\nolimits_{1,2}^r(E) - \sum\nolimits_{1,2}^a(E)] = -2\operatorname{Im}(\sum\nolimits_{1,2}^r(E)).$$

(18)

2.1. Numerical results and discussion

The (11, 0) semi-conducting nanotube, is very long with 235 unit cells and length $L = 100.11$ nm, and metallic leads have 2000 unit cells. The interface of (12, 0)-(11, 0) is composed of a pair pentagon-heptagon topological defect in the hexagonal network of the zigzag configuration. On-site energies are $\varepsilon_j = 0$ and hopping terms $\gamma_0 = -2.7$ eV.

The electronic properties of the metal-semiconductor (12,0)-(11,0) junction are illustrated in figure 1. The lower part of this figure shows the local density of states of interface. The Fermi energy coincides with the atomic π level, taken as zero of energy.

Analyzing the whole metallic-semi-conducting junction of figure 1 illustrates how the density of states around Fermi energy varies from ring to ring along the (12,0)-(11,0) connection. Moving from the starting ring 1 towards the first ring of the junction (ring 3), one can see the oscillation of the density of states, around the value of the plateau, calculated for the (12,0)-isolated nanotube. The DOS oscillations take place over a large range distance in front of the junction. Away from the junction, after rings 6, the local DOS will reduce and tends to zero, at the Fermi energy. In a planar hexagonal network, even-membered rings are neutral, five-membered rings are attractive, and seven-membered rings are repulsive of electrons [7]. Close to the interface, there is a finite LDOS in the gap of the semiconductor due to interface states. These states decrease with the distance from the interface. Several peaks around ± 1 eV, can be attributed to discrete states confined between the two interfaces.

The (12,0) nanotube is metallic, with a finite density of states at Fermi energy. As shown in figure 2, the DOS of this nanotube presents a plateau which extends 1 eV on both sides of the Fermi level, indicating the existence of one-dimensional metallic energy bands. The energies of the eigenstates are within $|E| \leq 3\gamma_0$ (-2.7 eV), which is consistent with three C-C bonds from each carbon atom. The (11,0) nanotube is a semi-conductor with a band gap of 0.6 eV. In both isolated nanotube, densities of states show many sharp peaks coming from the inverse square-
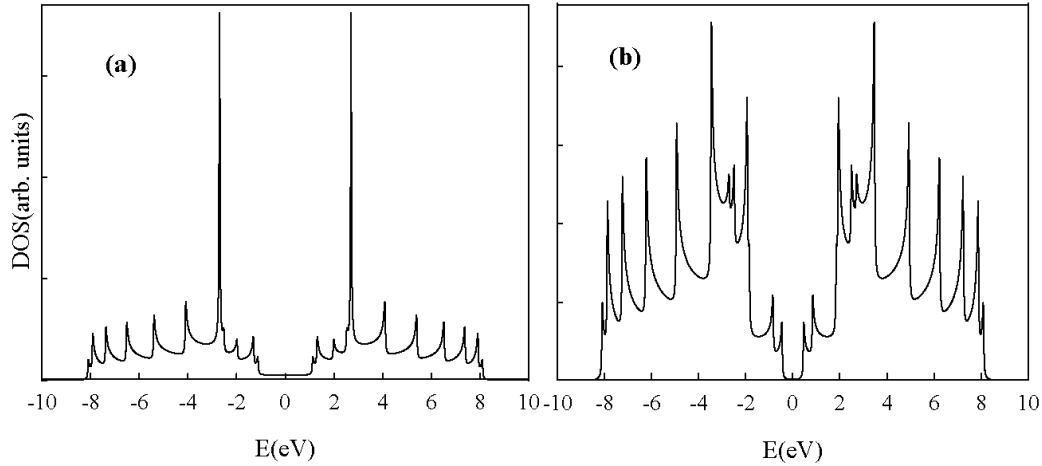
Figure 2. Densities of states in the isolated (12,0)-metallic and (11,0)-semiconducting nanotubes are illustrated in the right and left parts of the figure, respectively. All these curves are obtained from the recursion method. Small imaginary part is $\eta = 0.02$ eV.
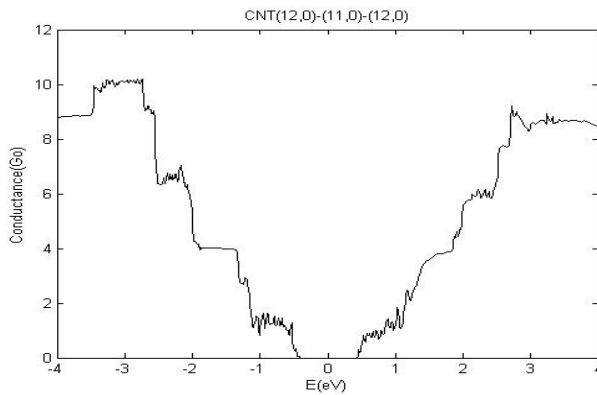

Figure 3. Conductance of the carbon nanotube (12,0)–(11, 0)–(12, 0).

Figure 4. Circuit diagram for carbon nanotube metal-semiconductor-metal.

root divergence of the spectra of the one-dimensional bands. These singularities are due to the quantization of the 1D energy bands in the circumferential direction.

In figure 3, we see small oscillations of the conductance around $E = \pm 1$ eV that are similar to the peaks observed in the LDOS. These oscillations correspond to states localized in the semi-conducting section. These localized states behave as point scatterers in the electronic transmission process.

3. A circuit model for carbon nanotubes

In the next step, we introduce a circuit model for the electrical properties of carbon nanotube metal-semiconductor-metal as figure 4. The high frequency circuit model [24] developed here, may have direct applications in determining the speed of switching for a variety of nanotube based electronic devices.

In this model, the kinetic inductance is given by [24]:

$$L = \frac{h}{2e^2 v_f} \approx 16nH / \mu m .$$ (9)

The combination of the quantum capacitance and the electrostatic capacitance in series has an equivalence capacitance of $C = 33aF / \mu m$ and the resistance of the
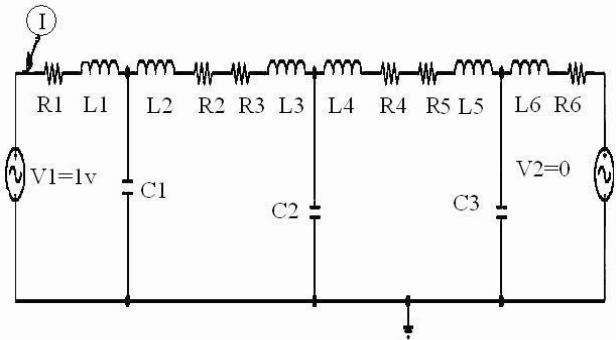
system is $R_{1,2,\dots,6} \approx 6.01\,k\Omega$. The effective voltage is 1V. The (11, 0) section, contains ten unit cells each has $L = 4.2$nm.

Figure 5 shows results of our circuit simulation using PSPICE software. This figure shows that the current is $27.73\,\mu A$, at the frequencies less than 53 MHz, while for example, at the frequency of 100 G Hz, the current reduces to $4\,\mu A$.

4. Conclusion

On the basis of the tight-binding model and Green's function method, we have studied the electronic structure and transport properties of a carbon nanotube metal-semiconductor-metal. In this formalism, and linear response regime, the electron transmission probability of the system at the Fermi energy is obtained.

We found that the local density of states at Fermi energy decrease with moving to semi-conducting section. Our numerical simulations for CNTs metal-semiconductor –metal show that the small oscillations of the peak positions are very intense at energy about 1eV. This effect can be contributed to the confined states between two interfaces. In other word, this peaks
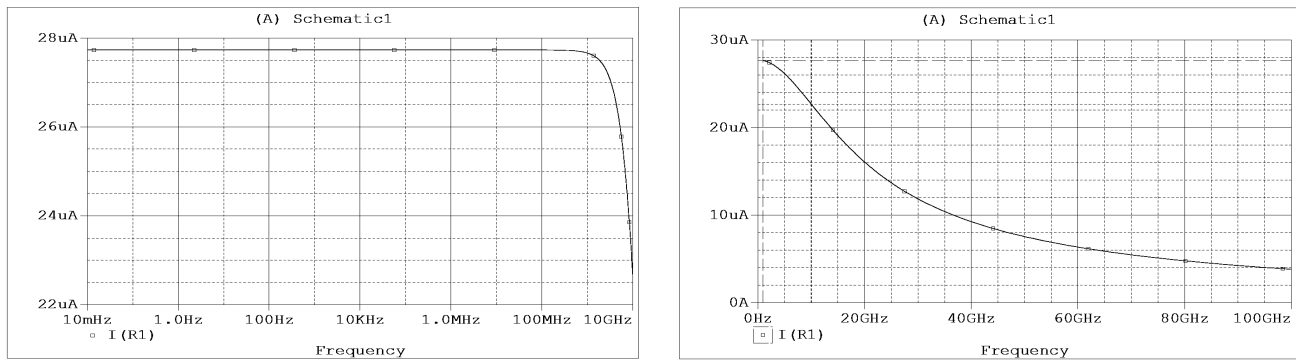
Figure 5. plots of current versus frequency for the circuit; the right part shows the behavior of current for the frequencies larger than 10 GHz .

correspond to the localization of electronic states of semiconductor. Semi-conducting nanotube behaves like a quantum box in which the distances between discrete energy levels will reduce with increasing its length. Also we found that the effect of the increasing in the frequency causes strong reduction in current. The

sensitivity of the system in the high frequencies is a suitable tool in the filtering for nano devices. Our calculations can be generalized to magnetic disorder embedded the wire, which can be act as a spin-filter, and also can be applied to the magnetic and nonmagnetic superlattices and multi-layers.

References

1. S Iijima, *Nature*, **354** (1991) 56.
2. S G Lemay, et al., *Nature,* **412** (2001) 617.
3. L CVenema et al., *Science,* **283** (1999) 52.
4. B I Dunlap, *Phys. Rev.* B **46** (1992) 1933.
5. R Saito, G Dresselhaus and M S Dresselhaus, *Phys. Rev.* B **53** (1996) 2044.
6. L Chico, V H Crespi, L X Benedict, S G Louie and M L Cohen *Phys. Rev.Lett.* **76** (1996) 971.
7. J C Charlier, T W Ebbesen and Ph Lambin, *Phys. Rev.* B **53** (1996) 11108.
8. M S Ferreira, T G Dargam, R B Muniz and A Latge, *Phys. Rev.* B **62** (2000) 16040.
9. R Tamura and M Tsukada, *Phys. Rev.* B **55** (1997) 4991.
10. H Kim, J Lee, S J Kahng, Y W Son, S B Lee, C K Lee, J Ihm and Y Kuk, *Phys. Rev. Lett.* **90** (2003) 216107.
11. A AOdintsov, *Phys. Rev. Lett.* **85** (2000) 150.
12. T Yamada, *Appl. Phys. Lett.* **80** (2002) 4027.
13. L Chico, L X Benedict, S G Louie and M L Cohen, *Phys. Rev.* B **54** (1996) 2600.
14. M Buongiorno Nardelli, *Phys. Rev.* B **60** (1999) 7828.
15. A Rochefort and Ph Avouris, *Nano Lett.* **2** (2002) 253.
16. L Chico, M P Lopez Sancho and M C Munoz, *Phys. Rev. Lett.* **81** (1998) 1278.
17. S Datta, *Electronic Transport in Mesoscopic Systems,* Cambridge: Cambridge University Press, (1995).
18. F Guinea, J Sanchez-Dehesa and F Flores, *J. Phys. C:Solid State Phys.* **16** (1983) 6499.
19. M P Lopez Sancho, J M Lopez Sancho and J Rubio, *J. Phys. F: Met. Phys.* **14** (1984) 1205.
20. M P Lopez Sancho, J M Lopez Sancho and J Rubio *J. Phys. F: Met. Phys.* **15** (1985) 851.
21. L Rosales, et al., *Phys. Rev.* B **75** (2007) 165401.
22. M Buttiker,Y Imry, R Landauer and S Pinhas, *Phys. Rev.* B **31** (1985) 6207.
23. Y Meir and N S Wingreen, *Phys. Rev. Lett.* **68** (1992) 2512.
24. P J Burke, *IEEE Trans. On Nanotech*, **2** (2003) 55.